

Multi-Target Search in Euclidean Space with Ray Shooting (Full Version)

Ryan Hechenberger, Daniel Harabor, Muhammad Aamir Cheema,
Peter J Stuckey, Pierre Le Bodic

Faculty of Information Technology, Monash University, Australia
{Ryan.Hechenberger, Daniel.Harabor, Aamir.Cheema, Peter.Stuckey, Pierre.LeBodic}@monash.edu

Abstract

The Euclidean shortest path problem (ESPP) is a well studied problem with many practical applications. Recently a new efficient online approach to this problem, RAYSCAN, has been developed, based on ray shooting and polygon scanning. In this paper we show how we can improve RAYSCAN by carefully reasoning about polygon scans. We also look into how RAYSCAN could be applied in the single-source multi-target scenario, where logic during scanning is used to reduce the number of rays shots required. This improvement also helps in the single target case. We compare the improved RAYSCAN⁺ against the state-of-the-art ESPP algorithm, illustrating the situations where it is better.

Introduction

Euclidean shortest path finding (ESPP) has many variants. We examine obstacle-avoiding 2D shortest (i.e. optimal) path determination, which is a well-studied problem with many practical applications, in e.g. robotics and computer games (Algoor, Sunar, and Kolivand 2015). Obstacles are an effective way to represent the world directly, for example, a wall can be represented as a rectangular obstacle that has to be navigated around.

ESPP algorithms can be very fast in *static* environments, i.e. where obstacles do not change between shortest path queries, as this allows for longer pre-processing. Search queries in a *dynamic* environment are considerably harder, as the obstacles change regularly, therefore any pre-processing has to be updated to account for these changes.

Most existing approaches to ESPP first convert obstacles into another representation to perform a search, either via a visibility graph (Lozano-Pérez and Wesley 1979) or a navigation mesh (Cui, Harabor, and Grastien 2017) for example. A recent approach is RAYSCAN (Hechenberger et al. 2020). It partially builds a visibility graph on the fly by using ray shooting (also called ray *casting*) to discover blocking obstacles, and then scanning along the edges of such obstacles to find ways around. RAYSCAN is comparable to an on-the-fly partial edge generation of a sparse visibility graph (SVG) running taut A* (Oh and Leong 2017); as such it does

This is the full version of an extended abstract released The 14th Annual Symposium on Combinatorial Search (SOCS 2021).

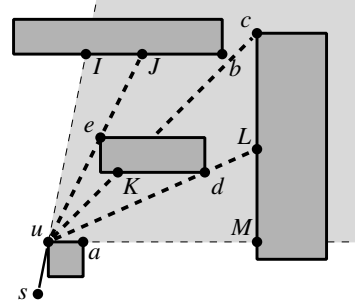


Figure 1: Expanding of node u

not require pre-processing, as it makes use of the natural polygonal representation of obstacles. Much of the runtime of RAYSCAN is taken up by the ray shooting.

In this paper we extend RAYSCAN with various improvements that are aimed at reducing the number of ray shots required. We call this advancement RAYSCAN⁺. We also tackle the multi-target variant, where we find the shortest path from a start point s to all target points $t \in T$.

We compare RAYSCAN⁺ against the state-of-the-art ESPP algorithm Polyanya (Cui, Harabor, and Grastien 2017); including tests with static and dynamic environments, single- and multi-target search. We show RAYSCAN⁺ significantly improves upon RAYSCAN and that RAYSCAN⁺ is competitive with Polyanya (in particular in highly dynamic scenarios).

RayScan

RAYSCAN is presented in this paper as a 2D ESP algorithm, made to work with a 2D environment represented as a set of non-intersecting polygonal obstacles (**inner-obstacles**), and a single enclosing polygon (**enclosure** or **outer-obstacle**), containing and non-intersecting all inner-obstacles. The **outer-boundary** is defined as the convex hull of the enclosure.

RAYSCAN does not provide the method of searching, rather it can be viewed as a fast method of producing a subset of edges of the visibility graph during the search. It uses the A* algorithm (Hart, Nilsson, and Raphael 1968) to drive the search, using **start** (s), **target** (t) and corner points on the polygons as the nodes in the search. When pushing a succes-

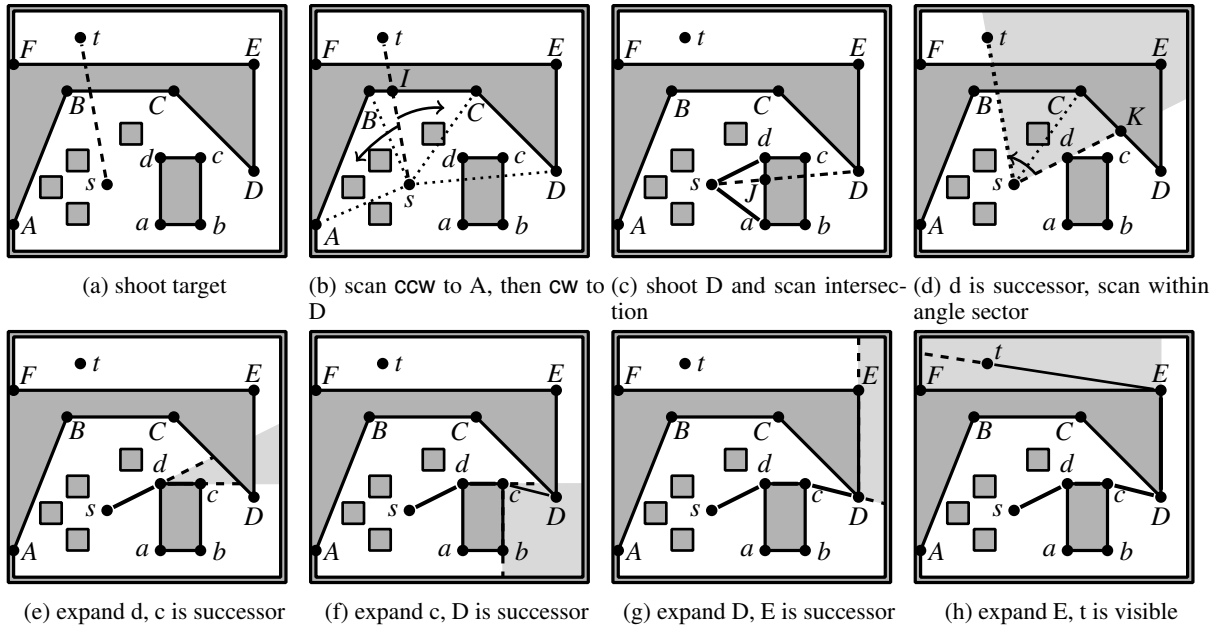


Figure 2: RAYSCAN Example (Hechenberger et al. 2020) - A dashed line is a ray shot. Each corner scanned by RAYSCAN is shown by a dotted line from s to the corner. The solid lines show the shortest path.

sor edge \vec{uv} , the edge weight is the Euclidean distance from u to v , $|\vec{uv}|$.

During the search, we expand nodes by producing successors. The search is directed with the heuristic function $h(v) = |\vec{vt}|$. We use the minimum f value to select the next node to expand, where $f(v) = g(v) + h(v)$ and $g(v)$ is the g value (length of the shortest path from s to v).

The search is directed by ray shooting, where a ray is shot from the expanding node u along a direction vector, which returns the first polygon hit by the ray and its intersecting point. This gives us an obstructing obstacle that we need to navigate around, which in a 2D environment, is restricted to two ways, clockwise (CW) or counter-clockwise (CCW).

The approach to navigate around an obstacle is the **scan** routine, where we trace a scan line along the polygon in a CW or CCW orientation w.r.t. expanding node u , e.g., Figure 1 shoots ray from u to c , finding intersection K ; a CW-scan starts from the scan line uK and has it sweep in a CW direction along polygon edge to point d and then stop, finding the d point which we refer to as a **turning point**. The CCW-scan has the scan line reach turning point e . Determining which point is considered a turning point can be done with two different approaches: the forward- and convex-scanning methods; that are detailed under the Scanning section. If there are no obstacles between u and a turning point, it is considered a **visible point** and is a successor node of u , otherwise it is a **blocked point**.

The scanning process does not end at finding the turning point; it instead recurses into new scans. Referring to Figure 1, for a blocked point like c , the scan will split into two scans, one CW the other CCW starting at the intersection point K . For a visible point like d (found from intersection K), we add d as a successor and shoot the ray past the point to find

the next polygon up (intersection L); then we continue the scan in the same orientation (CW) from that intersection (L). The whole recursive process starts from a single scan, where we call the whole process the **full scan**.

The recursive scanning process makes use of angled sectors to improve performance and as a base condition of the recursion. An angled sector is depicted as $AS(a_{ccw}, a_{cw})$, where the angled sector is defined as the angular region starting from the CCW pivot angle a_{ccw} , turning CW towards angle a_{cw} . Referring to Figure 1, the shaded area circular to uI and uM is an angled sector ($AS(uI, uM)$). During a scan, the scan line must always remain within this area; if at any point the scan line leaves the sector, the recursion ends with no (additional) turning point discovered. For the start point we abuse notation and use a 360° angled sector $AS(\vec{st}, \vec{st})$.

An angled sector can also be split into two angled sectors. We use the notation $SPLIT(AS(a_{ccw}, a_{cw}), \vec{p}, d)$ to split the angled sector $AS(a_{ccw}, a_{cw})$ along \vec{p} , returning a d -split (CCW-split or CW-split). The CCW-split returns $AS(a_{ccw}, \vec{p})$, while a CW-split returns $AS(\vec{p}, a_{cw})$. This split is used by the recursive scanning, where for turning point p , any recursive CCW scan will take the CCW-split of the current angled sector along p , and vice versa for CW scan.

Every expanding node u (excluding s) has a special angled sector known as the projection field. This angled sector encompasses the region that all successors of u must fall within, since any shortest path via u must be taut to the obstacle that u is part of. In Figure 1, the projection field for u is $AS(\vec{su}, \vec{ua}) \equiv AS(uI, uM)$. The full scan begins with the projection field, resulting in significant speedups by limiting the area the scan runs in.

A point on a polygon is considered to be a **concave point**

if its inside angle is more than 180° , otherwise is a **convex point**. Expanded nodes, with the possible exception of s , will always be convex, as you can only bend around such points.

RayScan Example

Consider the example execution of RAYSCAN illustrated in Figure 2 from (Hechenberger et al. 2020). Initially we expand s by shooting a ray from start s to target t (Figure 2a). We find this is blocked by a polygon (the outer polygon). We then recursively scan to move around the blocking polygon from I (Figure 2b). Scanning CCW we skip B since the ray cannot bend around the polygon here and reach node A which is on the convex boundary of the map, so we stop the scan. There is no way around the (outer) polygon in this direction. Scanning CW we skip C and reach D . We then shoot a ray towards D , which is blocked by the polygon $abcd$ at intersection J (Figure 2c). We recursively scan this polygon. The CW scan will find a as a turning point, shooting to it reveals it is visible and adds to the queue, and shooting past it will hit the outer-boundary, thus the CW scan does not continue. The recursion in the other orientation, CCW, finds turning point d , shooting to it and adding it to the queue (Figure 2d). We shoot past d and find intersection K , scan CCW from here we leave the angled sector boundary \vec{st} , ending the recursion.

Next we expand d (Figure 2e). The target is not within the projection field $AS(\vec{sd}, \vec{dc})$ so we scan both extreme edges. We shoot a ray \vec{dc} and find that c is visible from d , thus c is added as its successor. We scan the polygon that blocks \vec{dc} in CCW and leave the angled sector without discovering any turning point and stop. The other extreme ray \vec{sd} does not discover any successor. Next, we expand c in the same manner as d (Figure 2f), scanning CW to find only D . The next lowest f value is a , which we expand to find b (not shown in figure). Node b is then expanded (not shown in figure) and it finds D , although a shorter path to D is already discovered thus it is not added. Now, we expand D and find E scanning CW (Figure 2g).

Finally, we expand E and notice that t is within the projection field (Figure 2h), thus we shoot to t . We find that t is visible from E , thus we have found a path to t . This path is the shortest path because the node E had the minimum f value which guarantees that all other paths to t are no shorter than this path.

RayScan Improvements

The first contribution is a number of improvements to RAYSCAN. They do not change the underlying algorithm, but improve components hence the proof of optimality of RAYSCAN continues to apply.

Scan Overlap

The expansion of a node in RAYSCAN relies on multiple full scans, two from both ends of the projection field, called the **projection scans** (for any expanding node not s), and

an additional two if the target is within the projection field, called the **target scans**.

These full scans usually overlap with each other, resulting in redundant work of up to three complete scans of the region. We introduce two methods for reducing this overlap.

Refinement by sector: The first method, implemented in RAYSCAN, *refinement by sector*, works by refining the initial angle sector given to the full scan. Normally, the angled sector for the full scan is the projection field for projection scans, and the projection field split by \vec{ut} (where u is expanding node) for target scans. When we do a full scan that will overlap a previous scan for that expansion, work will become redundant when the scan line passes a ray shot by a previous full scan. To avoid this, we want to identify the closest CW or CCW to the starting scan line and split the angled sector to prevent the scan from passing it.

For example, in Figure 1, starting with a projection scan CW from \vec{su} , it starts with the angled sector of the projection field $AS(\vec{su}, \vec{ua})$, shoots the rays from u along \vec{su} , \vec{ub} , \vec{ue} and \vec{ud} . The next full scan starting CCW from \vec{ua} will have a reduced angled sector of the projection field $AS(\vec{ud}, \vec{ua})$.

Refinement by ray: The second method, implemented in RAYSCAN⁺, *refinement by ray*, uses the projection field for all full scans, instead ending a scan early when we try shooting a ray towards a turning point that we have already shot to this expansion.

For example, in Figure 1, as in the previous example we perform expansion of the first projection scan firing rays \vec{su} , \vec{ub} , \vec{ue} and \vec{ud} , out of these we shot rays towards turning points b , e and d . The full scan from \vec{ua} will find point c , shoot towards it and then recurse to find turning points e and d , which we have already shot rays to from a previous scan this expansion, thus both scans will end.

Scanning

Forward scan: The scan is split into two types, CW and CCW. The original RAYSCAN method uses a scan line that rotates in the specified orientation until the line is forced to turn the opposite way when encountering a polygon vertex. This is a turning point. We call this the *forward scan* method.

The idea of a turning point is to find a possible point that is visible from the expanding node and also on the shortest path. The forward scan method can find a concave point, which can never be on a taut path and hence not on any shortest path. We also know that a concave turning point can never be visible due to the nature of the scan, if the scan line goes from CCW to CW and is concave, the progressing line must be blocking the point.

For example, consider Figure 3a, point C , D and E are concave points, when performing a CW scan from ray \vec{st} , a forward scan will stop at E (as E to F orientates CCW) and shoot a ray. We see that E is blocked by its own polygon, though it will find F and H after the recursive scan.

Convex scan: We consider an alternate scanning method we call *convex scan*, where we only shoot at convex points, which are the only points that can appear on a shortest path. Referring back to the previous example, the scan line will instead pass over E even though it goes **opposite** to the scan-

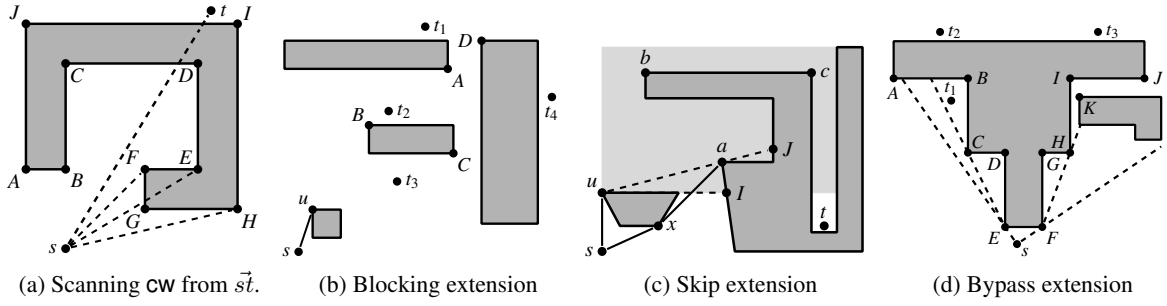


Figure 3: Auxilliary diagrams

ning orientation, as E is concave, instead resulting in finding F as a turning point.

Normally when we find a turning point (in this case F), and it is a visible turning point, we will shoot the ray past that point and recurse the scan in the same orientation. For the example CW scan we will normally then perform another CW scan, though this will simply reach F again. We can see that F is a turning point in the opposite orientation to the scan direction. We refer to this kind of point as a **backward turning point**. Given a visible-backward turning point we must recursively scan in the opposite orientation *and* continue the scan past F . For a CCW scan from $s\vec{F}$ ray (will go past the $s\vec{t}$ angled sector) and a CW scan will continue (go past G and end on H). This CW scan finds H , which is a **forward turning point**, and is handled as normal.

Avoiding Ray Shooting

RAYSCAN can be improved by avoiding shooting rays that are unnecessary. We list three different methods.

Blocking extension: Originally, RAYSCAN starts expanding a node u with the target scans (if t is within u 's projection field), followed by the projection scans. It is possible to instead start with the projection scans followed by target scans. The *blocking extension* makes use of this switch in the order of the full scans to potentially avoid some target scans entirely. If during the projection scans, we see that the target is not visible (i.e. is blocked by an obstacle edge we scanned over), then we do not have to shoot the target.

For example, in Figure 3b, we show several possible targets $t_{\{1,2,3\}}$. Expanding node u will shoot ray $s\vec{u}$ from u and do a CW scan to find A . During that scan t_1 is passed by the scan line behind the obstacle scanned, meaning we do not need to shoot to it later. After shooting to A , a CCW scan to find B , sees that t_2 is blocked, while a CW scan will find C and pass over t_3 , except in this case t_3 is in front of the obstacle so we still need to shoot towards it.

Skip extension: The *skip extension* attempts to skip (scan) past a turning point that cannot be on the shortest path. We can deduce a skip candidate point v from u if the following condition holds: $g(u) + \|\vec{uv}\| > g(v)$. Formally, expanding u , when finding a turning point v that has been reached by another point x , then $g(v) = g(x) + \|\vec{xv}\|$, and if the g value u will give v as a successor $g(u) + \|\vec{uv}\|$ is larger than v 's current g value, then this point may be skipped, as we know that candidate point v is not on a shortest path via

u . But we may need to find a shortest path to a point past v so the scan may need to continue.

For example, referring to Figure 3c, the shortest path is $s - u - b - c - t$. When expanding u , we perform a CCW-projection scan that starts at intersection I , then finds turning point a . We normally shoot to a and continue the CCW scan from J , except in this case we notice a has a shorter path from s via x . Since we do not want to reach a from u but need to continue the scan to find the successor on the shortest path b , we want to avoid shooting the ray to a . Instead, we continue the scan without shooting, ignoring all turning points (if any). If the scan line orientation reaches what would be the ray ($u\vec{a}$) when reaching J without leaving the angled sector (as is the case in this example) then we deduce that we do not need to shoot to a and can continue the CCW scan from J to eventually find the turning point b . Unlike this example, if we are unable to pass ray $u\vec{a}$, either from leaving the angled sector, reaching a again or encountering a certain number of points (a limit for performance reasons), then we *must* shoot to a to continue the scan. In any case, the scan must be continued CCW from J as b is on the shortest path from u .

Bypass extension: The final extension outlined in this paper is the *bypass extension*, which is similar to the skip extension except it can be applied to turning points that are not skip candidates, which do not appear that often. Bypass seeks to skip shooting a ray to a node in the same way as the skip extension, except it also checks if the scan line sweeps over the target, and if it does not then we can bypass the node. For example; with Figure 3d, when expanding E , the CCW projection scan reaches C and attempts to bypass it. The scan line will continue from C past B before reaching the ray that would be $E\vec{C}$; if t_1 is our desired target then the scan line sweeps over it, meaning we cannot bypass C (as it is on the shortest path); if however t_2 is our desired target; although we sweep past it, we did not sweep over t_2 as it is blocked by the polygon, thus we can bypass C , which is done the same way as skip. The scan then immediately leaves the angled sector producing no successors.

Sometimes a node on the shortest path will be bypassed when expanding another node on the shortest path; take Figure 3d as an example, when expanding node F ; we perform a CW projection scan that finds turning point H (on the shortest path), except the point can be bypassed, thus RAYSCAN⁺ will skip over it to find turning point J . This is where con-

sidering the angled sector is important, as that bypass was done with the projection field $AS(\vec{FG}, s\vec{F})$; however, since we did not shoot a ray to H that angled sector remains the same, this is important as it allows us to reach H further in the full scan. After find turning point J (on the shortest path), we shoot a ray and find it blocked, thus we recurse, the CCW scan will find turning point K (also on the shortest path), which if we can reach will get us to J . We shoot a ray to K to find it again blocked by line segment GH , which when we recurse scan CW will again find H , except this time in the check to bypass it, we have the angled sector $AS(\vec{FK}, \vec{FJ})$ and thus, trying to bypass will quickly leave the scan's angled sector along the line segment HI , therefore bypass has failed and we need to shoot to H .

Caching Rays Shot

The ray shots are the most expensive part of RAYSCAN, as we will show in the experimental sections; therefore, reducing the cost of these shots can achieve great performance improvements. We make use of a simple method of remembering rays we shoot so that subsequent queries that shoot the same rays can just look at the result.

For our method for caching rays, we store the results of a ray shot from node u to node v , where $u, v \notin \{s, t\}$. The dynamic cases changes the results of stored ray, thus any changes in the environment invalidates the whole cache, and we start again.

Extension to Multi-Target ESPP

RAYSCAN⁺ can be extended to support single-source multi-target searches. A naive way to do this is, during expansion, instead of looking for a single target within the projection field and shooting a ray, find all targets within the projection field and shoot rays to all. A change of the heuristic function $h(u)$ either to 0 or to the distance from u to the closest target maintains the admissibility of the heuristic.

The number of additional rays shot to every target significantly increases runtime, which can be counteracted by the target blocking extension.

Algorithm 1 details a successor generator for RAYSCAN⁺, modified from RAYSCAN to support multiple targets. It can find paths from a start node s to a list of target nodes T .

Function START_SUCCESSORS(s, T) (line 1) will generate successors for source node s that will lead to all targets T . Function SUCCESSORS(u, T, F) similarly finds successors for the expanding node u for all $t \in T$ within its projection field F .

Function POPULATE_TARGETS(T, F) (line 2 and 5) filters the list of targets T that are within projection field F and orders them circularly within the angled sector. These targets are stored within the TARGETS_REMAINING global variable.

Function SHOOTRAY(u, a) handles the ray shooting and returns the intersecting polygon p , the intersection point I , and a boolean R indicating if shot in direction a from u has already been made this expansion. Lines 23 to 25 check for all collinear points the ray intersects with, and pushes the closest visible one as successor (if present) (line 25). The ray

Algorithm 1 Generate u 's successors within projection field

```

1: function START_SUCCESSORS( $s, T$ )
2:   POPULATE_TARGETS( $T, AS(\vec{st}, \vec{st})$ )
3:   TARGET_SUCCESSORS( $s, AS(\vec{st}, \vec{st})$ )
4: function SUCCESSORS( $u, T, F = AS(a_{ccw}, a_{cw})$ )
5:   POPULATE_TARGETS( $T, F$ )
6:   ( $p, I, -$ )  $\leftarrow$  SHOOTRAY( $u, a_{ccw}$ )
7:   SCAN( $u, p, I, F, T, CW$ )
8:   ( $p, I, R$ )  $\leftarrow$  SHOOTRAY( $u, a_{cw}$ )
9:   if  $R$  is false then
10:     SCAN( $u, p, I, F, CCW$ )
11:   TARGET_SUCCESSORS( $u, F$ )
12: function TARGET_SUCCESSORS( $u, F$ )
13:   while TARGETS_REMAINING  $\neq \emptyset$  do
14:      $t \leftarrow$  any target in TARGETS_REMAINING
15:     REMOVE_TARGETS( $t$ )
16:     ( $p, I, -$ )  $\leftarrow$  SHOOTRAY( $u, \vec{ut}$ )
17:     if  $t$  is visible from  $u$  then
18:       PUSH_SUCCESSOR( $u, t$ )
19:     else
20:       SCAN( $u, p, I, F, CW$ )
21:       SCAN( $u, p, I, F, CCW$ )
22: function SHOOTRAY( $u, a$ )
23:   if ray hits one or more turning points then
24:      $n \leftarrow$  first turning point  $n$  hit
25:     PUSH_SUCCESSOR( $u, n$ )
26:   Let ( $p, I, R$ ) be the first polygon  $p$  blocking the ray
27:     at intersection  $I$ , and  $R$  if shot to  $a$  before
28:   return ( $p, I, R$ )
29: function SCAN( $u, p, I, F, d$ )
30:   scan  $p$  from  $I$  in direction  $d$  to find turning point  $n$ 
31:   REMOVE_TARGETS(targets blocked during scan)
32:   if scan leaves  $F$  then return
33:   if scan touches outer-boundary then return
34:   ( $p', I', R$ )  $\leftarrow$  SHOOTRAY( $u, \vec{un}$ )
35:   if  $R$  is true then return
36:   if  $n$  is visible from  $u$  then
37:     if  $n$  is a forward turning point then
38:       SCAN( $u, p', I', SPLIT(F, \vec{un}, d), d$ )
39:     else  $\triangleright n$  is a backward turning point
40:        $d' \leftarrow$  opposite orientation of  $d$ 
41:       SCAN( $u, p', I', SPLIT(F, \vec{un}, d'), d'$ )
42:       SCAN( $u, p, n, SPLIT(F, \vec{un}, d), d$ )
43:   else
44:     SCAN( $u, p', I', SPLIT(F, \vec{un}, CW), CW$ )
45:     SCAN( $u, p', I', SPLIT(F, \vec{un}, CCW), CCW$ )

```

will stop when it is blocked by an edge; if it only touches the corner of a polygon without entering (i.e. a collinear point) it will pass through it.

When expanding the start node s , we shoot to all the targets (line 3). The TARGET_SUCCESSORS(u, F) (line 12) will handle all the target scans by shooting from the expanding node u towards all remaining targets (when expanding node u is the start node, all targets are the remaining targets).

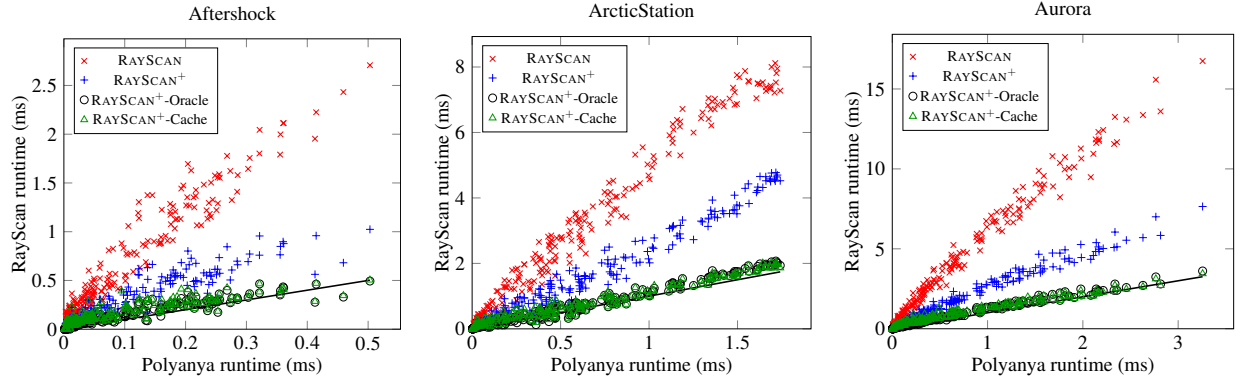


Figure 4: Scatter plots of Polyanya runtime vs RAYSCAN implementations for single target search

Algs	Aftershock	Aurora	ArcticStation
R	568	3604	2752
N	400	2548	2689
NB	388	2492	2627
NS	375	2392	2090
NP	262	1638	1859
NC	150	736	683
NBSP	248	1560	1395
NBSPC	132	723	625

Table 1: Comparing separate extensions (rows) on different maps (columns); single-target average runtime per query (all times are in μ s); (R) Original RAYSCAN; (N) convex scan RAYSCAN⁺; (B) blocking extension; (S) skip extension; (P) bypass extension; and (C) ray caching

The successors will continue to shoot to targets (lines 13 to 21). Specifically, it selects any of the remaining targets t (line 14), removes it from the TARGETS_REMAINING variable (line 15) and shoots towards it (line 16). If t is visible, it is pushed as a successor (line 18). Otherwise, the polygon that blocks the ray is scanned CW and CCW while potentially removing additional targets that are found to be blocked (lines 20 and 21).

Expanding any node u other than the start node will first do the projection scans by shooting along the extremes of its projection field F and scan inwards of F along the blocking polygon (lines 6 to 10) like RAYSCAN. Line 9 is the refinement by ray. These scans may have blocked some targets in TARGETS_REMAINING which are removed. The function TARGET_SUCCESORS(u, F) is called to shoot towards these remaining targets if any (line 11).

Function SCAN(u, p, I, F, d) is used to scan the polygon p which blocked a ray shot from u at the intersection point I . This function scans p starting at I in orientation d (CW or CCW) while restricted to the angled sector F . We first find a turning point by sweeping a line from I in orientation d to find a suitable turning point n (line 30). RAYSCAN⁺ uses convex scan to find a turning point whereas original RAYSCAN used forward scan. This scan also uses the blocking, skipping and bypass extensions and removes targets that

are found to be blocked during the scan (line 31).

If the scan leaves the projection field F or touches the outer-boundary, we terminate the scan (lines 32 and 33). Otherwise, we shoot a ray from u towards n (line 34). Refine by ray is enforced on line 35 to terminate the scan if a ray towards n was previously shot from u . If not, we recurse the scan, which differs slightly depending on whether n is visible from u (line 36) or not. Like original RAYSCAN, if the visible turning point is a forward turning point, we recurse the scan in the same orientation with a split angled sector (line 38). Otherwise, if it is a backward turning point, we recurse both ways, handling the opposite scan (lines 40 and 41) and continuing to find the next forward turning point (line 42). For a non-visible turning point, we follow the same principles as RAYSCAN in that we try to scan CW around the blocking point p (line 44) and CCW (line 45).

Experiments

The data set used for the experimentation stems from the Moving AI Lab pathfinding benchmarks (Sturtevant 2012). We make use of three representative Starcraft maps: Aftershock, ArcticStation and Aurora, which are converted from the grid representation to Euclidean polygonal obstacles.

These experiments were conducted on a machine with an Intel i7-8750H, locked at 2.2 GHz with boost disabled. Every search was run 7 times, discarding the best and worst results, then averaging the remaining 5. The source code will be made available¹.

Comparison against Original RayScan

The improvements listed in this paper can be seen in Figure 4, four different RayScan algorithms are compared against Polyanya. RAYSCAN shows the original RayScan implementation (Hechenberger et al. 2020), which uses the forward-scan method and refinement by sector (although it was not detailed in the paper). RAYSCAN⁺ uses an updated implementation using the convex-scan method with target blocking, skip and bypass extensions and refinement by ray. The RAYSCAN⁺-Oracle is the same as RAYSCAN⁺ except the shooting of rays cost comes for free. RAYSCAN⁺-Cache

¹<https://bitbucket.org/ryanhech/rayscan/>

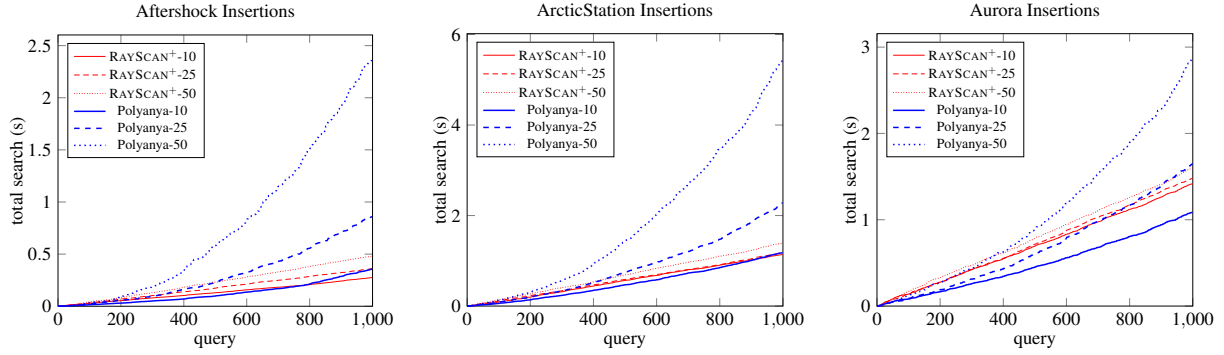


Figure 5: Dynamic accumulative search time (no setup) with varying number of inserts/removal of total obstacles every 10 single target instances

caches the results of ray shots from previous queries. The implementation of the ray shooting is done by drawing Bresenham’s lines on a grid (Bresenham 1965).

Our Polyanya implementation code is modified from the implementation by Cui, Harabor, and Grastien (2017). The navigation mesh was generated by constrained Delaunay triangulation (CDT) using Fade2D.² The triangle faces were greedily merged to make larger convex faces to improve Polyanya’s performance.

Figure 4 illustrates the significant advantages of RAYSCAN⁺ over RAYSCAN on single target problems. These results show that Polyanya is still faster for searching than RAYSCAN⁺ for static environments, but adding caching to RAYSCAN⁺ achieves very competitive results. The disadvantage of caching rays is that for large maps this can lead to higher memory usage, as the number of rays shot can be in the order of the number of edges in the SVG. In the case where memory usage gets too large, caching strategies can be employed to ensure the memory usage never exceeds a given budget.

Table 1 provides an ablation study of the extensions we propose. Caching is clearly the most important extension (since ray shots are the most expensive part of the algorithm). Each other extension has a positive effect, with bypass the most effective (since the environments we test on have many non-convex polygons) and blocking the least (for single targets). The positive effects combine so best is using all of them.

Dynamic Single Target Scenarios

We conduct experiments for dynamic environments with results shown in Figure 5. These tests show the accumulated runtime (y -axis) of the algorithms over 1000 queries (x -axis), where we insert or remove 10, 25 or 50 small convex polygons in the environment every 10 queries, while leaving the original map untouched (i.e. no polygon originally on the maps is modified).

Inserting obstacles into Polyanya’s mesh is done by splitting the faces the polygon lines intersect and constraining them. To remove them, we clear the constraint between the

faces along the obstacle edges. Polyanya also needs to find which face a point holds (for start, target and insert of new polygon). This is done by selecting a face and moving across the mesh in a direct line to the point.

Figure 5 shows that RAYSCAN⁺’s search performance is fairly consistent, as changes to its data structures are fast and do not degrade performance. Polyanya shows the performance is degrading as removing the obstacles is degrading the mesh; while this can be alleviated by repairing the mesh, this does incur additional costs in removal of unnecessary vertices and/or merging smaller faces together.

Polyanya’s performance degrades significantly as the environment is changed more rapidly, because the navigation mesh gets more and more complicated. Maintaining the mesh with methods by Kallmann, Bieri, and Thalmann (2004) that maintains the CDT or van Toll, Cook IV, and Geraerts (2012) that makes use of a Voronoi diagram become mandatory to maintain Polyanya’s performance. In highly dynamic maps RAYSCAN⁺ is faster.

Multi Target Scenarios

In Figure 6a-c, we consider multi-target scenarios where the targets are clustered fairly close together. We have two types of scenarios: Figure 6a and 6b split the Aurora map into 10x10 grid cells and randomly choose a number of different targets within one of those cells. Figure 6c evaluates the impact of a larger number of targets which are placed in a randomly chosen cell from a 6x6 grid.

Multi-target Polyanya makes use of the interval heuristic (Zhao, Taniar, and Harabor 2018), which produces a Dijkstra like expansion for Polyanya. This can impact the search performance in clustered examples since Polyanya is not actively seeking out the targets; however, Polyanya only needs to consider each target during the search when it reaches a face containing the target.

Using RAYSCAN⁺ for multiple targets makes heavy use of the blocking extension, as otherwise we need to shoot to all targets within the projection field of each node expanded, resulting in many additional rays. RAYSCAN⁺ uses the Euclidean distance to the closest target to the vertex. For a small number of targets (e.g. Figure 6a), the heuristic and selection of targets within each projection field is done by

²<https://www.geom.at/products/fade2d/>

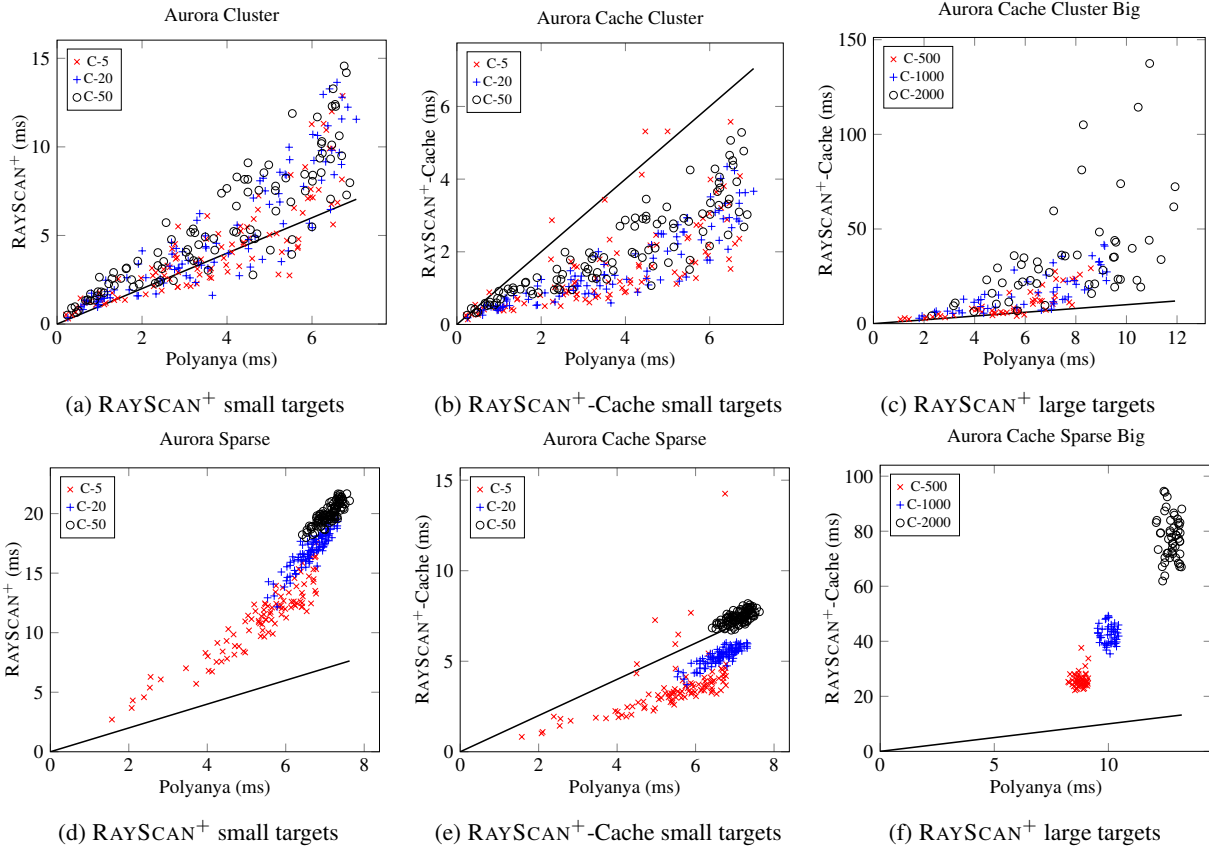


Figure 6: Multi-target tests on map Aurora; (a)-(c) are with clustered targets; (d)-(f) are with sparse targets. C- n details tests with n number of targets of Polyanya (x -axis) vs RAYSCAN+ (y -axis)

checking all targets. For larger number of targets (e.g. Figure 6c) we use a Hilbert R-Tree (Kamel and Faloutsos 1999) to speed up these calculations.

Examining Figure 6a, we see that for clustered targets Polyanya is fairly consistent as the number of targets change, compared to RAYSCAN+, which slows down as the number of targets grow. This is expected as Polyanya only needs to handle targets at the beginning (to locate each target's face) and the end (to finalise the path to target); whereas RAYSCAN+ needs to deduce for each node expansion which targets are in its projection field.

Figure 6b illustrates that when caching the rays, RAYSCAN+ is competitive with Polyanya. It is faster than Polyanya when the targets are clustered together. The high spikes for C-5 are early searches still building up the cache.

Figure 6c compares results for a larger number of targets. This highlights a weakness of RAYSCAN+ since it has to consider each target within its projection field for every expansion. RAYSCAN+ must do this as it only produces a subset of successors, which means vital successors needed to reach a target might not be found without shooting to that target from certain nodes. Until a method of addressing this weakness is found, RAYSCAN+ will struggle with very large numbers of targets compared to Polyanya.

Figure 6d-f compares the methods for sparse target points,

which are distributed at random around the map. The nearest point heuristic for RAYSCAN+ is less effective in these scenarios, resulting in RAYSCAN+ performance degrading more with each additional point, as the Polyanya interval heuristic is more useful in these cases. We see that the RAYSCAN+-Cache speeds perform slightly worse at 50 targets, but is highly competitive with fewer targets.

An ablation study shows that for multi-target blocking is an important extension: for 5-50 targets it leads to 20% improvements; for 500-2000 it can speed up by more than $2\times$.

Conclusion

RAYSCAN+ is an efficient method for Euclidean shortest path finding in dynamic situations, since it requires almost no pre-processing to run. In this paper we show how to substantially improve RAYSCAN+ by reversing the order of target and projection scans, and reducing the number of vertices we need to shoot rays at. We extend RAYSCAN+ to shoot at multiple targets. RAYSCAN+ is competitive with the state of the art ESPP method Polyanya when we cache ray shots, which make up the principle cost of RAYSCAN+. Future work will examine better methods to maintain ray shot caching in dynamic situations.

Acknowledgements

Research at Monash University is supported by the Australian Research Council (ARC) under grant numbers DP190100013, DP200100025 and FT180100140 as well as a gift from Amazon.

References

- Algfoor, Z. A.; Sunar, M. S.; and Kolivand, H. 2015. A comprehensive study on pathfinding techniques for robotics and video games. *International Journal of Computer Games Technology* 2015: 1–11. ISSN 1687-7047.
- Bresenham, J. E. 1965. Algorithm for computer control of a digital plotter. *IBM Systems journal* 4(1): 25–30.
- Cui, M. L.; Harabor, D.; and Grastien, A. 2017. Compromise-free Pathfinding on a Navigation Mesh. In *Proceedings of the 26th International Joint Conference on Artificial Intelligence*, 496–502. AAAI Press.
- Hart, P. E.; Nilsson, N. J.; and Raphael, B. 1968. A formal basis for the heuristic determination of minimum cost paths. *IEEE transactions on Systems Science and Cybernetics* 4(2): 100–107. ISSN 0536-1567.
- Hechenberger, R.; Stuckey, P. J.; Harabor, D.; Le Bodic, P.; and Cheema, M. A. 2020. Online Computation of Euclidean Shortest Paths in Two Dimensions. In *Proceedings of the 30th International Conference on Automated Planning and Scheduling*, 134–142. AAAI Press.
- Kallmann, M.; Bieri, H.; and Thalmann, D. 2004. Fully dynamic constrained delaunay triangulations. In *Geometric modeling for scientific visualization*, 241–257. Springer.
- Kamel, I.; and Faloutsos, C. 1999. Hilbert R-Tree: An Improved R-Tree Using Fractals. *Proceedings of the 20th International Conference on Very Large Data Bases* 500–509.
- Lozano-Pérez, T.; and Wesley, M. A. 1979. An algorithm for planning collision-free paths among polyhedral obstacles. *Communications of the ACM* 22(10): 560–570. ISSN 0001-0782.
- Oh, S.; and Leong, H. W. 2017. Edge N-Level Sparse Visibility Graphs: Fast Optimal Any-Angle Pathfinding Using Hierarchical Taut Paths. In *Proceedings of the Tenth International Symposium on Combinatorial Search (SoCS 2017)*.
- Sturtevant, N. 2012. Benchmarks for Grid-Based Pathfinding. *Transactions on Computational Intelligence and AI in Games* 4(2): 144 – 148. URL <http://web.cs.du.edu/~sturtevant/papers/benchmarks.pdf>.
- van Toll, W. G.; Cook IV, A. F.; and Geraerts, R. 2012. A navigation mesh for dynamic environments. *Computer Animation and Virtual Worlds* 23(6): 535–546. doi:10.1002/cav.1468. URL <https://onlinelibrary.wiley.com/doi/abs/10.1002/cav.1468>.
- Zhao, S.; Taniar, D.; and Harabor, D. D. 2018. Fast k-nearest neighbor on a navigation mesh. In *Eleventh Annual Symposium on Combinatorial Search*.